American Mineralogist, Volume 77, pages 631–642, 1992

An empirical phase diagram for the clinozoisite-zoisite transformation in the system $Ca_2Al_3Si_3O_{12}(OH)$-$Ca_2Al_2Fe^{3+}Si_3O_{12}(OH)$

GERHARD FRANZ

Fachgebiet Petrologie, Technische Universität Berlin, Straße des 17 Juni 135, D-1000 Berlin 12, Germany

JANE SELVERSTONE

Department of Earth and Planetary Sciences, Harvard University, 20 Oxford Street, Cambridge, Massachusetts 02138, U.S.A.

ABSTRACT

The effects of pressure, temperature, and $Fe^{3+} \rightleftharpoons Al$ exchange on the transformation from orthorhombic zoisite to clinozoisite are examined using thermodynamic data and analyses of naturally coexisting mineral pairs. Theoretical considerations indicate a steep transformation loop in the *T-X* sections, with the Al end-member reaction occurring at low temperature and the Fe end-member reaction at high temperature; the orthorhombic phase is the high-temperature form. The position of the two-phase zoisite-clinozoisite area in a *T-X* section varies with pressure. Equilibrium mineral pairs from low- to intermediate-pressure regimes indicate a smaller two-phase area (between approximately 8–15 mol% Al_2Fe in zoisite and 25–40 mol% in clinozoisite) than those from high-pressure regimes (same variation in zoisite, 35–55 mol% in clinozoisite). The width of the two-phase region also depends on minor elements, such as the rare earth elements. The effect on the phase diagram of a possible low-temperature miscibility gap in the monoclinic series is also discussed. Disequilibrium textures, such as complex zoning patterns and multiple generations of grains, are common features in naturally coexisting clinozoisite-zoisite pairs. Owing to the sluggish reaction behavior of the epidote minerals, these can serve as important petrogenetic indicators of prepeak or relict metamorphic conditions in a wide range of bulk compositions.

INTRODUCTION

The epidote mineral group, like the pyroxenes and feldspars, exhibits both chemical and structural variations. The principal isomorphous substitution $Al \rightleftharpoons Fe^{3+}$ is continuous over a wide range of compositions and operates in both orthorhombic and monoclinic crystals. The structural transformation from the orthorhombic to the monoclinic form thus potentially depends on pressure, temperature, and chemical composition. This transformation is petrologically significant in a variety of metamorphic environments: zoisite is part of the high-pressure assemblage that replaces lawsonite and anorthite and is common in many eclogites; epidote minerals are ubiquitous in mafic rocks throughout the blueschist, greenschist, and epidote amphibolite facies; and zoisite and clinozoisite both occur in calc-silicate rocks from a variety of *P-T* environments. Despite its petrologic importance, however, the effects of structural and chemical variations on reactions involving epidote group minerals are not well understood.

The controversy concerning the zoisite-clinozoisite phase diagram can be summarized as follows. Enami and Banno (1980) analyzed coexisting zoisite-clinozoisite mineral pairs from rocks of different metamorphic grade. They arranged the analyses by increasing metamorphic grade (i.e., temperature) and suggested that, with increasing temperature, both the monoclinic and the orthorhombic forms become enriched in Fe^{3+}. However, Ackermand and Raase (1973) observed that clinozoisite and zoisite showed prograde core to rim zoning toward Fe-poor compositions. Prunier and Hewitt (1985) presented experimental evidence that at high temperatures both forms are relatively Fe rich and thus verified Enami and Banno's hypothesis. Comparing the loop proposed by Prunier and Hewitt (1985) with the data of Enami and Banno (1980) still leaves considerable uncertainty about the exact position in *P-T* space of the two-phase loop and its form in *T-X* and *P-X* projections. The aim of this study is to present new data on coexisting zoisite and clinozoisite mineral pairs in order to construct an empirical phase diagram that stresses the important influence of pressure on the phase transformation.

THEORETICAL CONSIDERATIONS

This investigation is restricted to the system $Ca_2Al_3Si_3O_{12}(OH)$-$Ca_2Al_2Fe^{3+}Si_3O_{12}(OH)$; the influence of other potentially important substitutions involving Mn, Cr, and rare earth elements is only briefly discussed. In addition, we restrict it to the Al-rich part of the system, where only up to one-third of the total Al is replaced by Fe^{3+} (and we assume that Fe^{2+} is not important). Higher Fe contents are only rarely reported in the literature (e.g.,

0003–004X/92/0506–0631$02.00

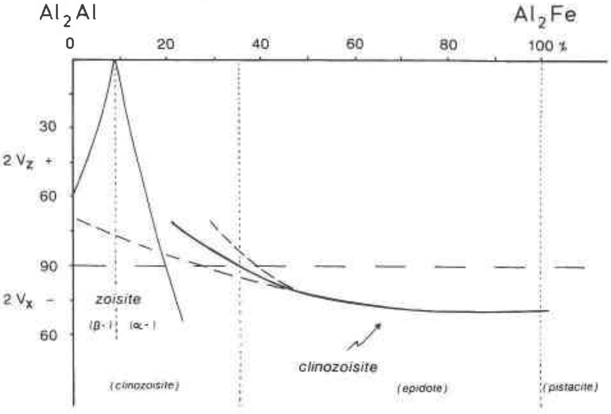

Fig. 1. Nomenclature of the epidote group minerals in the system $Ca_2Al_3Si_3O_{12}(OH)$-$Ca_2Al_2FeSi_3O_{12}(OH)$. Orthorhombic zoisite includes the Fe-poor variety β zoisite with orientation of the optic axial plane parallel to (010) and the Fe-rich variety α zoisite with the optic axial plane parallel to (100). Monoclinic zoisite includes clinozoisite proper, which is optically positive, epidote proper (optically negative), and the hypothetical composition pistacite (not shown), $Ca_2Fe_3Si_3O_{12}(OH)$. Because of the high optic axial angle dispersion of the epidote minerals and the strong effect of minor elements on optical properties, the exact position of the curves varies (dashed lines, diagram modified after Tröger, 1982; Maaskant, 1985).

Bird et al., 1988) and appear to be confined to low-temperature environments; these monoclinic high-Fe epidote samples have not been reported coexisting with an orthorhombic member of the epidote series and hence are not relevant to the problem addressed here.

We use the following nomenclature, which is based on optical properties and summarized in Figure 1. Zoisite is the orthorhombic form. The optical varieties with different optic axial orientations and a change from positive to negative character (see Myer, 1966; Vogel and Bahezre, 1965; Maaskant, 1985), which is strongly dependent on Fe content, are considered as one phase, since there is no indication that these chemical (and optical) variations are discontinuous or that they are related to structural discontinuities. There is also no clear indication of structurally different types in the monoclinic series (Deer et al., 1986). A continuous range of compositions from low to high Fe contents exists at certain *P-T* conditions, and the monoclinic series can also be represented by one phase. We use the term "clinozoisite" throughout this paper to refer to monoclinic forms and reserve "epidote" for the whole mineral group; "pistacite," which is also a term used for Fe-rich epidote, may be used for the hypothetical end-member $Ca_2Fe_3Si_3O_{12}(OH)$. The Fe-free monoclinic end-member is known from experimental studies (e.g., Jenkins et al., 1985). Several studies on natural samples suggest that miscibility gaps occur within the monoclinic series (Hietanen, 1974; Raith, 1976; Selverstone and Spear, 1985). These proposed miscibility gaps are located at relatively high Fe contents of the system or have a rather low critical temperature or both. Their possible influence is discussed in a subsequent section.

The transformation from monoclinic to orthorhombic forms can be described in terms of two end-member reactions:

$$\text{mcl } Ca_2Al_3Si_3O_{12}(OH) = \text{orh } Ca_2Al_3Si_3O_{12}(OH) \quad (1)$$

$$\text{mcl } Ca_2Al_2FeSi_3O_{12}(OH) = \text{orh } Ca_2Al_2FeSi_3O_{12}(OH). \quad (2)$$

The structures of the orthorhombic and monoclinic forms are similar. They consist of SiO_4 and Si_2O_7 groups linked by octahedral chains occupied by Al and Fe^{3+}. The two forms are related to each other by a glide-twin operation, but the types of octahedral chains in the two forms are essentially different: in zoisite only one type of chain occurs, whereas in clinozoisite there are two types of chains (Dollase, 1968). The transformation can also be described as cation shuffle or synchroshear (Ray et al., 1986) with a rearrangement of (Al,Fe) and Ca on the M3 site. Such a transformation is probably of first order with a two-phase region in a *T-X* or *P-X* section. It cannot be described as a miscibility gap, which would be a function only of cation ordering. In the epidotes, ordering of octahedrally coordinated Al and Fe^{3+} is almost complete in zoisite (Fe^{3+} in the Al3 site; Ghose and Tsang, 1971) and less perfect in clinozoisite (Fe^{3+} in the M3 site, with small amounts in the M1 site; Dollase, 1971).

Both Enami and Banno (1980) and Prunier and Hewitt (1985) argued that pressure has no influence on the transformation loop, owing to the very small difference in molar volumes of the orthorhombic and monoclinic forms (V_{zoi} = 135.9 cm^3/mol, V_{clz} = 136.2 cm^3/mol, Helgeson et al., 1978; V_{zoi} = 135.58, V_{clz} = 136.73, Holland and Powell, 1990; V_{zoi} = 135.88, V_{clz} = 136.76, Berman, 1988). However, the *P-T* slope of a reaction depends on both ΔV and ΔS, and since the entropy values for the epidote minerals are also similar (S_{zoi} = 296.1 J/K·mol, S_{clz} = 295.7 J/K·mol, Helgeson et al., 1978; S_{zoi} = 295, S_{clz} = 291, Holland and Powell, 1990; S_{zoi} = 297.58, S_{clz} = 287.08, Berman, 1988; S_{zoi} = 296.58, S_{clz} = 294.06, Gottschalk, 1990), it is possible that pressure exerts a significant effect on the position and shape of the two-phase region. The reported molar-volume value with the smallest error in determination of the lattice constants for synthetic orthozoisite was given by Langer and Lattard (1980) as 135.77 cm^3/mol, which is in good agreement with the data from the above mentioned data sets. No reliable data for synthetic Fe-free clinozoisite are known. Pistorius (1961) reported identical values for zoisite and clinozoisite (within the limits of error) of 136.4 ± 0.7 cm^3/mol. Extrapolation of data for Fe-bearing clinozoisites presented by Myer (1966), Bird and Helgeson (1980), and Seki (1959) yields a value of 136.2 cm^3/mol. Linearly extrapolated data from Hörmann and Raith (1971) indicate a slightly higher value of 136.5, but they suggest that a linear extrapolation is probably not correct, and their given line would extrapolate toward a value of 137.5 cm^3/mol.

Reaction 1 has a negative slope in *P-T* space, although there is a large range in the magnitude of the slope obtained with different data sets (−124 bars/°C, Berman, 1988; −13.3 bars/°C, Helgeson et al., 1978; −34.8 bars/°C, Holland and Powell, 1990). If an average value of −50 bars/°C is accepted, a pressure increase of 2 GPa would shift the equilibrium temperature for Reaction 1 by 400 °C. No thermodynamic data for Reaction 2 are available. If we assume that the change in entropy arising from the exchange of Fe^{3+} for Al is essentially the same regardless of whether the exchange occurs in an orthorhombic or a monoclinic crystal, the *P-T* slope of Reaction 2 depends only on the molar volumes and the entropy contribution from order-disorder phenomena. Bird and Helgeson (1980) compiled data on lattice constants and calculated molar volumes. In their Figure 2 it can be seen that, with increasing Fe^{3+} contents, the difference in the molar volumes of the orthorhombic and monoclinic forms may get smaller.

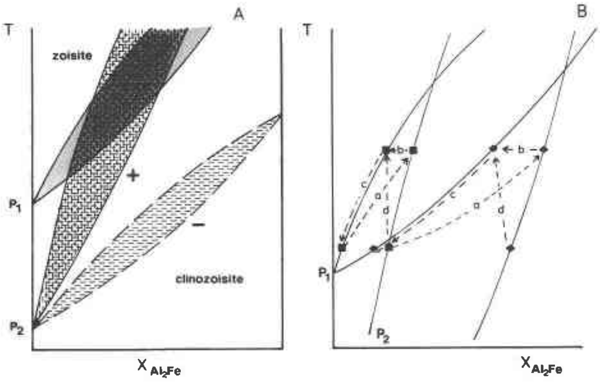

Fig. 2. Schematic *T-X* phase diagram for the transformation from clinozoisite to zoisite. (**A**) The two possibilities of either a positive (+) or a negative (−) *P-T* slope for the Al_2Fe end-member Reaction 2 for two isobaric sections at low pressure *P*1 and high pressure *P*2. (**B**) An enlarged part of A, showing the possible zoning trends of coexisting minerals (squares = zoisite, diamonds = clinozoisite) during prograde and retrograde development (paths a–d, see text). The range of compositions of the orthorhombic and the monoclinic types during such a cycle may overlap, and Fe-poor clinozoisite may therefore coexist with relatively Fe-rich zoisite in complexly zoned minerals.

If there is significant order-disorder of Al and Fe in the epidotes, it is likely that the degree of disorder in clinozoisite is higher than in zoisite (Dollase, 1971; Ghose and Tsang, 1971), which results in a decrease in ΔS for Reaction 2. Bird and Helgeson (1980) give an entropy difference for ordered-disordered epidote of 0.3 J/K·mol. Changing the value of ΔS and a decreasing ΔV will have a large effect on the slope of the reaction, but unfortunately uncertainties in the available entropy and volume data and lack of data concerning their sensitivity to substitution and order-disorder phenomena do not allow us to distinguish with confidence between a positive and negative slope for Reaction 2.

For the construction of a schematic *P-T-X* diagram, it is also necessary to have some information about the temperature range in which Reactions 1 and 2 are located. Jenkins et al. (1985) determined Reaction 1 experimentally and located it at temperatures below 350 °C; calculations with the data of Berman (1988) yield a temperature near 200 °C at 1 bar. Despite the uncertainties in the absolute temperatures, there is no doubt that the orthorhombic form is the high-temperature form. Reaction 2 is probably metastable because it must lie at temperatures well above 600 °C. This was demonstrated experimentally by Holdaway (1972) and empirically by the common occurrence of monoclinic epidote near its upper stability limit in amphibolite facies rocks.

Figure 2 shows *T-X* sections for Reactions 1 and 2, with the assumption of both positive and negative slopes for Reaction 2 and extreme temperature differences between the two reactions. In a *T-X* diagram the limbs of the two-phase region are very steep, and their position changes with pressure and the changing slope of Reaction 2. If a negative slope for Reaction 1 is correct, it is clear that pressure has a large effect on the composition of coexisting phases. With the assumption that the model with a positive slope for Reaction 2 is correct, coexisting zoisite and clinozoisite would exhibit different types of zoning, depending upon the *P-T* path they had followed during metamorphism: a simple prograde path with simultaneous burial and heating would result in increasing Fe contents from core to rim of both phases (path a in Fig. 2B), whereas isothermal uplift (path b) and isobaric cooling (path c) would result in decreasing Fe contents; heating during uplift (path d) would also cause a rimward decrease in Fe content of both minerals. If Reaction 2 has instead a negative *P-T* slope, the two-phase region is shifted with increasing pressure toward lower temperatures. Qualitatively, the change in composition of coexisting pairs would be the same for the *P-T* paths discussed for Figure 2B, but the change would be much more pronounced for both minerals, in contrast to the small changes in zoisite composition illustrated in Figure 2B.

NATURALLY COEXISTING ZOISITE-CLINOZOISITE PAIRS

In order to constrain the position of the two-phase region, we analyzed coexisting minerals from a variety of *P-T* regimes. This approach has some inherent problems. The first problem is that epidotes, especially Fe-rich clinozoisite, can preserve extremely complicated zoning patterns, which show up clearly in backscattered electron images and indicate slow diffusion rates at metamorphic temperatures. In theory, slow Fe^{3+}-Al diffusion should make the epidote minerals suitable for an empirical study of the two-phase region because their sluggish reaction behavior inhibits retrograde reequilibration. In practice, however, epidotes can form over a wide range of *P-T*

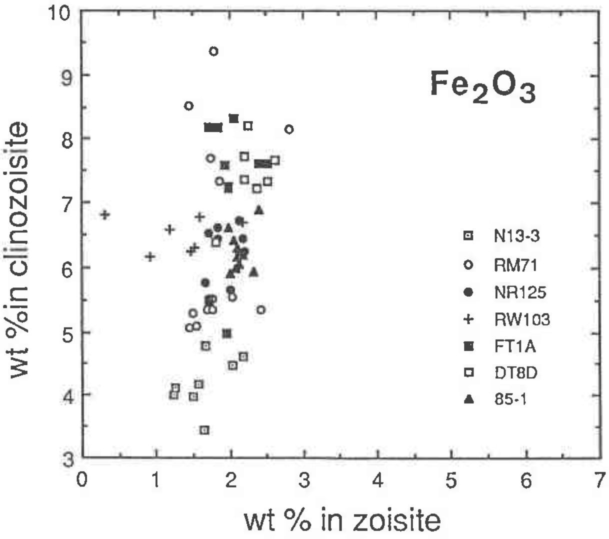

Fig. 3. Distribution of Fe_2O_3 between clinozoisite and zoisite (only analyses of grains in contact with one another are plotted); clinozoisite is strongly enriched in Fe_2O_3.

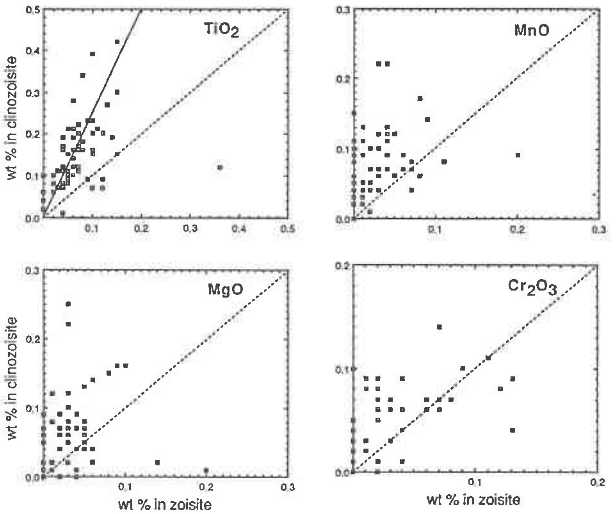

Fig. 4. Distribution of the minor components TiO_2, MnO, MgO, and Cr_2O_3 between clinozoisite and zoisite (same data set as Fig. 3; overlapping analyses not shown). The 1:1 slope line is given as a reference line; for TiO_2 a reference line with a slope of 2.5:1 is also shown.

conditions between the lower greenschist facies and the eclogite facies, which at times makes it difficult to determine if coexisting zoisite and clinozoisite grew during the same event. We selected grains that appeared to belong to the same fabric generation and worked with backscattered electron images to analyze only grains in mutual contact and with no evidence for late-stage growth or reequilibration.

Uncertainties in the microprobe analyses give rise to an error on the order of ±1 mol% Al_2Fe. Assuming an error of 0.1 absolute wt% for an Fe-bearing zoisite with 1.75 wt% Fe_2O_3 results in ±0.6 mol% Al_2Fe. An error of 1.25 relative wt% in SiO_2 has no influence on the calculated Al_2Fe component, whereas an error of 1.25 relative wt% in Al_2O_3 results in ±0.3 mol% Al_2Fe. The presence of minor elements such as Cr or Mn results in only a slight overestimation of the Al_2Fe component. In most of the analyses the sum of minor octahedral cations per formula unit is below 0.05, which has little influnce on the mol% Al_2Fe, calculated as $100[Fe_{tot}/(-2 + Al_{tot} + Fe_{tot})]$.

All analyses were carried out with automated Camebax electron microprobes at Harvard University and the Technische Universität Berlin, with simultaneous energy-dispersive analysis to check for minor elements, and with backscattered electron images to avoid mixed analyses on adjacent grains or on different zones within the grains. Despite different standards and correction programs (Harvard—natural minerals, Bence-Albee correction; TUB—natural minerals and synthetic metals, PAP correction), analyses on the same materials are identical in the range mentioned above.

Distinction between orthorhombic and monoclinic crystals was made in thin section by determination of the extinction angle in grain sections showing the *a*-*c* plane. In most samples, other optical features, such as anomalous interference colors, crystal shape and size, and inclusion patterns, were also helpful in distinguishing between zoisite and clinozoisite. Additional transmission electron microscopy was done on two samples; a detailed report on this work is in preparation (Smelik and Franz).

Compositions of coexisting phases

The Fe_2O_3, TiO_2, MnO, MgO, and Cr_2O_3 contents of all coexisting clinozoisite-zoisite pairs from all rock types are given in Figures 3 and 4. All analyses are compiled in Table 1.[1] Figure 3 shows that Fe_2O_3 is preferentially incorporated into the monoclinic form. TiO_2 (Fig. 4) is also preferentially incorporated in clinozoisite, up to a maximum value of 0.4 wt%. MnO and MgO are also enriched in clinozoisite (up to 0.2 wt%), whereas Cr_2O_3 partitioning behavior is unclear (Fig. 4). Preferential incorporation of the minor elements into the monoclinic crystals will contribute to the uncertainty in position and slope of the two-phase loop in the Al-Fe system, but because the absolute amounts are small, they are probably of minor importance. This is not the case, however, if these elements are present in large amounts, as is demonstrated for the rare earth elements. Sample BP 119 (metagranite from the Granatspitzkern Zentralgneis, Tauern Window, Austria; Fig. 5) contains zoisite blasts with small (approximately 20-μm) clinozoisite inclusions, which have variable amounts of REE. The zoisite has a constant composition with 6–8 mol% Al_2Fe, but the Fe

---

[1] Table 1 may be ordered as Document AM-92-496 from the Business Office, Mineralogical Society of America, 1130 Seventeenth Street NW, Suite 330, Washington, DC 20036, U.S.A. Please remit $5.00 in advance for the microfiche.

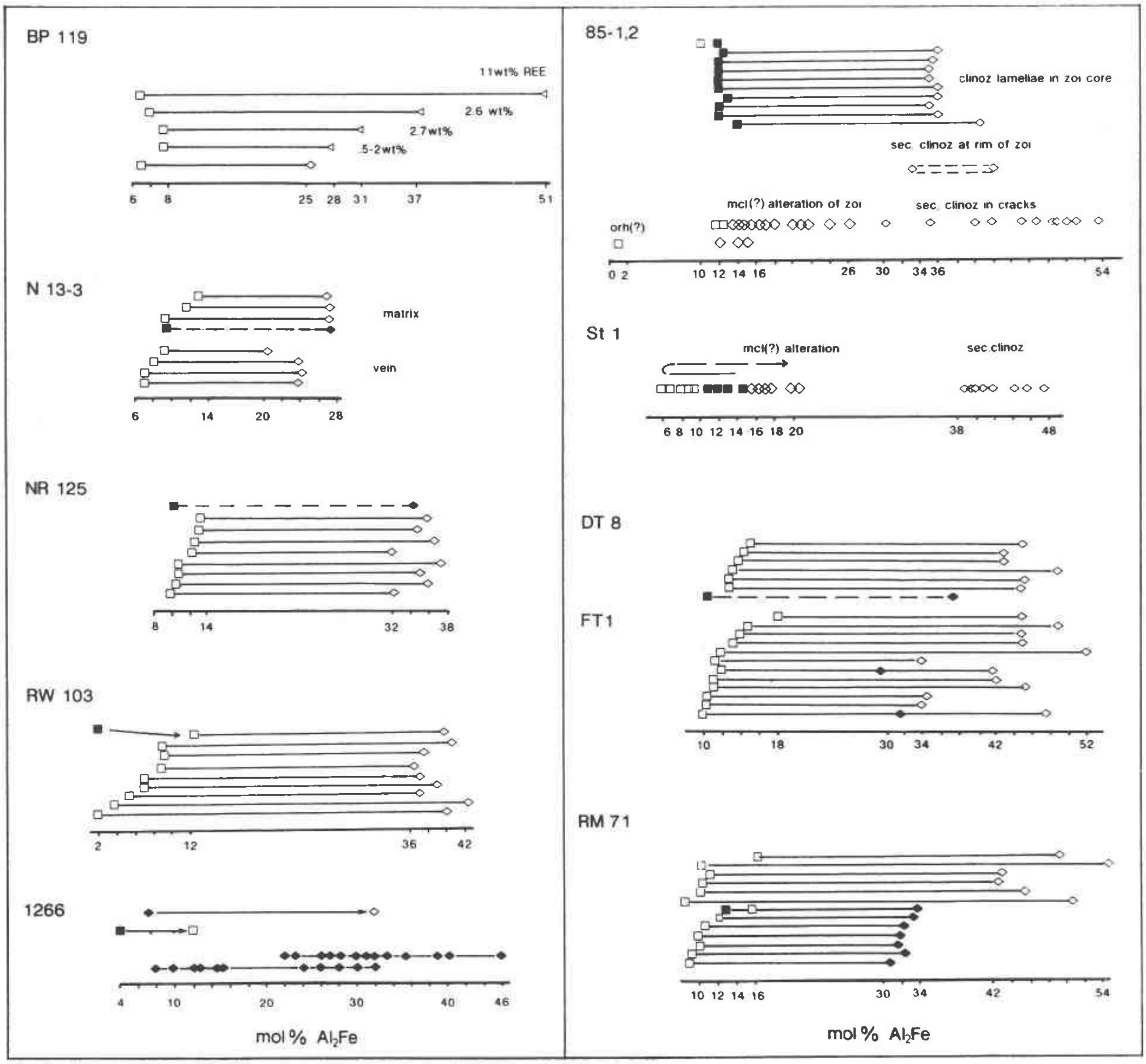

Fig. 5. Analytical results for the investigated samples of clinozoisite-zoisite pairs; squares = orthorhombic; diamonds = monoclinic; rotated squares = structural state uncertain; triangles = rare earth–bearing clinozoisite. Lines connect coexisting minerals; analyses were made a few micrometers away from the grain boundary. Sample BP 119: REE-bearing and REE-free inclusions of clinozoisite in zoisite; the width of the two-phase area widens with increasing REE content. N 13-3: Matrix and vein assemblage in a low-grade amphibolite; filled symbols indicate core compositions. Sample NR 125: Tourmaline-epidote segregation from contact metamorphic environment; filled symbols indicate core compositions. Sample RW 103: Calc-silicate nodule from a polymetamorphic granulite to amphibolite facies terrane. Solid symbol indicates Fe-poor granulite facies zoisite with overgrowth of Fe-richer zoisite during amphibolite facies metamorphism. Sample 1266: Low-grade calc-silicate rock. Closed and open squares represent core and rim analyses, respectively, of grains determined optically to be orthorhombic; closed and open diamonds are core and rim analyses from clinozoisite, with a continuous range of intermediate compositions (no analysis points shown). Closed diamonds (lower two rows) represent monoclinic intergrowths (two crystals determined with TEM) that contain 8–32 mol% Al_2Fe in one case and 22–46 mol% Al_2Fe in the other. The compositional gap between 15 and 24 mol% in one crystal does not indicate a miscibility gap, since microprobe analyses of other crystals fall into this range. Samples 85-1 and 85-2: Pegmatoid vein in eclogite with formation of clinozoisite in core of zoisite, secondary clinozoisite near and at the rim of zoisite, secondary clinozoisite in cracks in zoisite. The samples show both equilibrium and disequilibrium pairs and also the alteration of primary zoisite into clino(?)zoisite with increasing Fe contents. Newly formed crystals with ≤ 1 mol% Al_2Fe are too small for structural determination; an orthorhombic structure is consistent with the proposed phase diagram, but not proved. Sample St 1: Quartz-zoisite vein from eclogites, showing the same type of alteration of primary zoisite as in samples 85-1 and 85-2. Core compositions of the zoisite (filled symbols) is Fe rich, rims are Fe poor, but near to alteration products Fe content increases. Samples DT 8 and FT 1 are from eclogites, filled symbols indicate core compositions. Both clinozoisite and zoisite show a wider range of compositions compared to the low-*P* rocks. Dashed line connects core compositions of two adjacent crystals. Sample RM 71 is an epidote + garnet + albite vein in an eclogite. The high Fe rim of clinozoisite is only 5–10 μm wide (open diamonds), inside of this rim (filled diamonds) the clinozoisite is homogeneous.

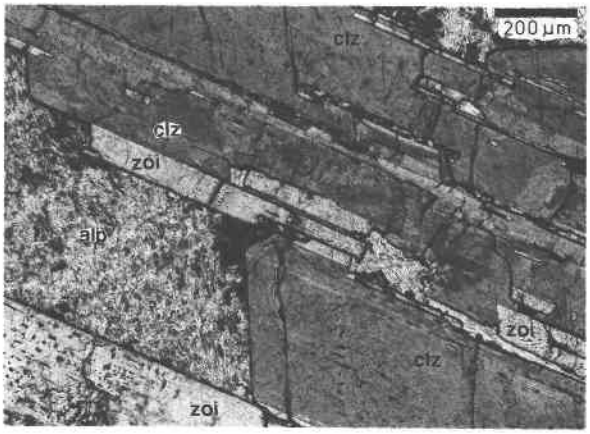

Fig. 6. Photomicrograph of equilibrium intergrowth of clinozoisite (34–36 mol% Al_2Fe) in the core of a zoisite (12 mol% Al_2Fe), together with (sericitized) albite (sample 85-1, crossed polars).

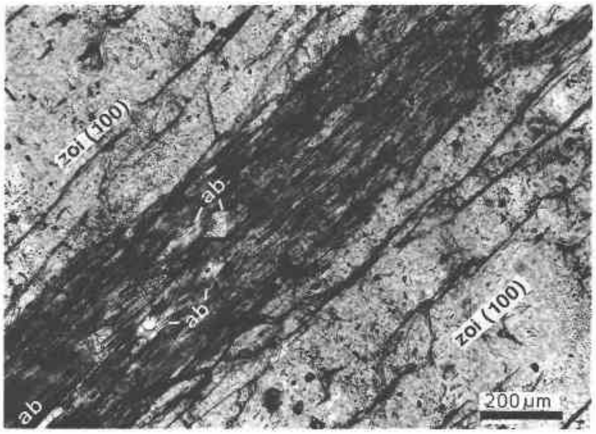

Fig. 7. Photomicrograph of zoisite with 10–12 mol% Al_2Fe with alteration zones parallel to (100) (dark because of anomalous interference colors) with 15 mol% Al_2Fe, intergrown with albite (ab; sample 85-1, crossed polars).

content in the clinozoisite varies from 25 mol%, where the REE are below the detection limit (0.5 wt%), to 51 mol%, where the REE total is 11 wt% (estimated from Ca deficiency and deviation of ideal anhydrous total of 98.5 wt%; semiquantitative energy dispersive analysis). The REE end-member of the epidote group, allanite, contains Fe^{2+} in large proportions (Dollase, 1971), and therefore these high Fe contents do not reflect the true Al_2Fe mol%, and clinozoisite of this type cannot be used to constrain the two-phase loop.

Petrographical description

Owing to the problems mentioned above (complex zoning, growth at different *P-T* conditions) each sample is different and must therefore be described separately.

Sample N 13-3 (Fig. 5) comes from an ophiolite complex in the Gebel Rahib area, Darfur, northwestern Sudan (Abdel Rahman et al., 1990). T_{max} and P_{max} are roughly estimated for this area as 400 ± 50 °C and <0.5 GPa, respectively, from the mineral assemblage amphibole + chlorite + epidote + plagioclase + quartz + calcite. Retrograde shearing in the rocks is recorded by transformation of amphibole with 6 wt% Al_2O_3 into actinolite with 3 wt% Al_2O_3. The sample shows coexisting zoisite and clinozoisite in the matrix and in a small, deformed veinlet. In the matrix, both minerals have the same grain size and morphological features and show only minor variation in chemical composition from core to rim. In the veinlet, zoisite is larger in grain size than clinozoisite and shows sector zoning (variation from 5 to 9 mol% Al_2Fe). In the veinlet, coexisting mineral pairs are zoisite with 7–9, clinozoisite with 20–25 mol% Al_2Fe, compared to matrix zoisite with 9–14 mol% and clinozoisite with 27–28 mol% Al_2Fe.

Sample NR 125 (Fig. 5) is a tourmaline-epidote segregation. It comes from the contact of a granitoid with metasediments, the so-called Hüllserie ("Seetörl" locality, Granatspitz Zentralgneiskern, Tauern Window, Austria). Although these rocks subsequently underwent Tertiary Alpine metamorphism, the Paleozoic contact metamorphism is well preserved and is characterized by the mineral assemblage calcite + wollastonite + quartz + grossular + diopside. Temperatures near 550 °C at 0.2 GPa are assumed to represent the equilibration conditions. There is no significant zoning in the epidote minerals, and tourmaline inclusions in the epidote cores are similar in composition as the matrix tourmaline crystals. Zoisite contains 10–13 mol% Al_2Fe, clinozoisite 32–37 mol%.

Samples 85-1 and 85-2 (Figs. 5, 6, 7) are quartz-albite(An_{10})-zoisite-phengite segregations in the Weissenstein eclogite, Münchberg Massif (Germany). The eclogite itself formed at high pressures of at least 1.9 GPa at temperatures near 620 °C (Klemd, 1989). The segregations and associated pegmatoids probably formed during uplift when the *P-T* path just crossed the minimum melting curve (Franz et al., 1986) at pressures of approximately 0.9 GPa. Crystallization of a granitic melt at these conditions yields zoisite and potassium white mica instead of potassium feldspar and anorthite component (Johannes, 1985). Within the centimeter-sized zoisite crystals are 0.1-mm-wide lamellae of clinozoisite (Fig. 6) together with pure albite; the lamellae have straight grain boundaries, typically occur in the cores of the zoisite crystals, and are oriented parallel to (100) of zoisite. They are interpreted as equilibrium intergrowths that formed during cooling of the segregations. The zoisite crystals are zoned with rims slightly lower in Fe content (10 mol% Al_2Fe) compared to the cores (12–13 mol%). Coexisting mineral pairs give consistent values of 12–13 mol% Al_2Fe and 35–36 mol%, with one exception (14 and 41 mol%). Texturally similar clinozoisite located at the rim of the large zoisite crystals shows a larger variation in Al_2Fe content from 35 to 42 mol%.

A second type of clinozoisite (with 31–53 mol% Al_2Fe) occurs along irregular cracks in zoisite (see Fig. 9 in Hammerschmidt and Franz, 1992) and also parallel to (100) and (010) planes of the host zoisite (Fig. 7), where it is accompanied by a slight change in interference colors of the adjacent zoisite. The clinozoisite formation and modification of the zoisite took place at a later stage, probably below 350 °C at low pressure. A late (postmetamorphic) hydrothermal stage that might have been responsible for the features shown in Figure 7 has been documented by Hammerschmidt and Franz (1992) for the Münchberg Massif. The modified zoisite crystals vary between 12 and 26 mol% (analyses at points where interference colors changed or immediately adjacent to the secondary clinozoisite). We were unable to determine by optical methods whether these crystals are monoclinic or orthorhombic, but preliminary transmission electron microscopy results show deviations from orthorhombic symmetry in these areas (a detailed description of these results will be presented elsewhere). We were also unable to determine the symmetry of small crystals approximately 5 μm in diameter that are located in the albite matrix parallel to (100) of zoisite (Fig. 7) and in altered pegmatitic plagioclase next to the pegmatitic zoisite crystals. These small crystals have Al_2Fe contents near 1 mol%. Assuming that the latter are orthorhombic and the zoisite modifications are monoclinic, a compositional gap between 1 and 12 mol% exists. The rocks from this locality provide an excellent example of the variety of epidote minerals that form during cooling. Only the primary intergrowths were used in determination of the transformation loop, although the secondary clinozoisite crystals give some constraints about the position of the loop at low *P* and *T*.

Sample 1266 (Figs. 5, 8) is also from the Münchberg area, but from the border zone adjacent to very low-grade sediments (locality Schwingen, near Schwarzenbach/Saale, Germany). This so-called prasinite-phyllite series did not experience temperatures in excess of 350 °C (the stable assemblage is stilpnomelane + actinolite + chlorite + calcite + albite; pressures are not determined, but there is no indication of high pressures). The specimen is a calcite-phengite rock with minor amounts of epidote, titanite, and tourmaline, from a greenschist-metapelite contact. Zoisite occurs as needle-shaped crystals 5–20 μm, with 4–12 mol% Al_2Fe mostly restricted to the calcite-rich part of the sample, whereas large clinozoisite grains (300 μm) with 7–46 mol% Al_2Fe occur mainly in the phengite-rich part of the sample. They were not found in clear grain contact but were within a few micrometers of each other. Closer inspection of these crystals with backscattered electron images revealed zoning from core to rim toward Fe-rich compositions in both the monoclinic and the orthorhombic grains, although zoning in the clinozoisite was less regular (Fig. 8). The monoclinic nature of those parts of the crystals with very low Fe content (8 mol%, determined by analytical electron microscopy) was verified by selected area diffraction analysis of two crystals. The analyses clearly demonstrate that, at low *P-T* conditions, low to intermediate Al_2Fe clinozoisites exist, indicating that there is no obvious miscibility gap, and that there can be an overlap in compositions of zoned clino- and orthozoisite that grew during a prograde burial and heating event.

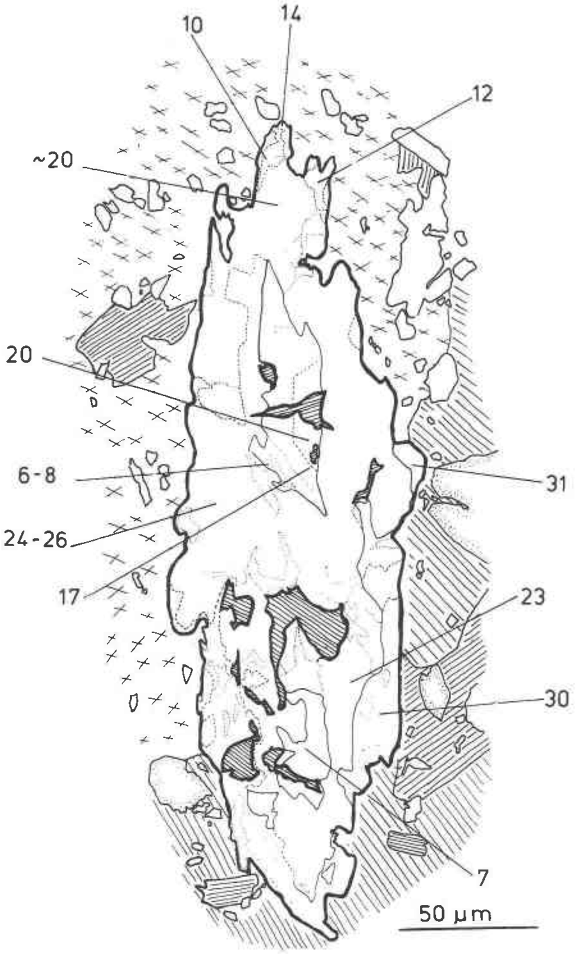

Fig. 8. Zoning in clinozoisite (drawing after backscattered electron image, sample 1266) in a calcite + phengite matrix (cleavage indicated) showing central compositions with low Fe content (6 mol%, as indicated in the figure) increasing toward the rim in irregular zones (separated in the figure by dotted and solid lines according to their sharpness) up to 31 mol%; all intermediate compositions were found. Some of the Fe-rich zones have REE present in small amounts. Small crystals are zoisite, ranging from 4 to 12 mol% Al_2Fe from core to rim, and subordinate titanite (stippled).

Sample St 1 (Fig. 5) is another example of modifications to primary zoisite during retrograde development. This sample comes from the eclogite zone (Knappenhaus locality, Frosnitztal, Tauern Window, Austria), from a zoisite-quartz segregation in a banded eclogite (Thomas and Franz, 1989). Following eclogite facies metamorphism, these rocks underwent subsequent alteration in the *P-T* range from the lower amphibolite facies down to temperatures below 350 °C (Spear and Franz, 1986). The

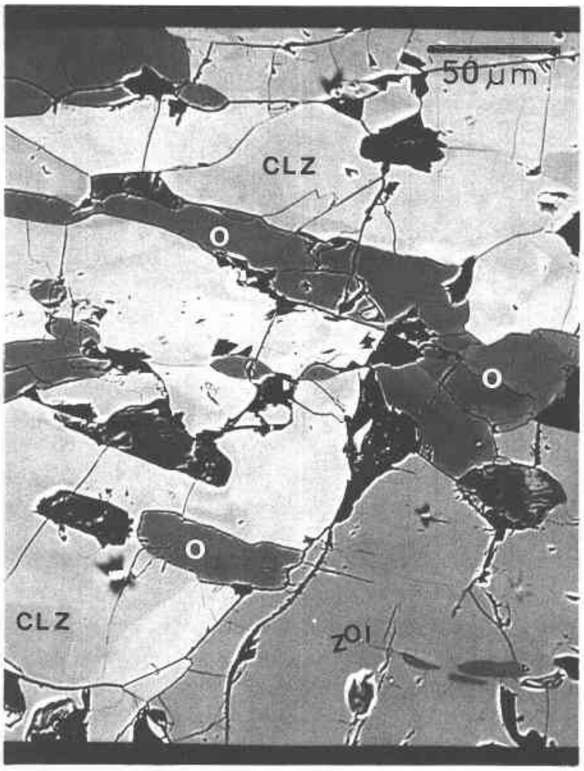

Fig 9. Backscattered electron image of clinozoisite and zoisite from eclogites equilibrated at 2 GPa (sample DT-8), together with omphacite (O) and amphibole (black, not labeled). The omphacite crystal in the lower left grows across the grain boundary between zoisite and clinozoisite and also across the core (Fe poor, 37 mol% Al_2Fe) and the rim (Fe rich, 49 mol% Al_2Fe).

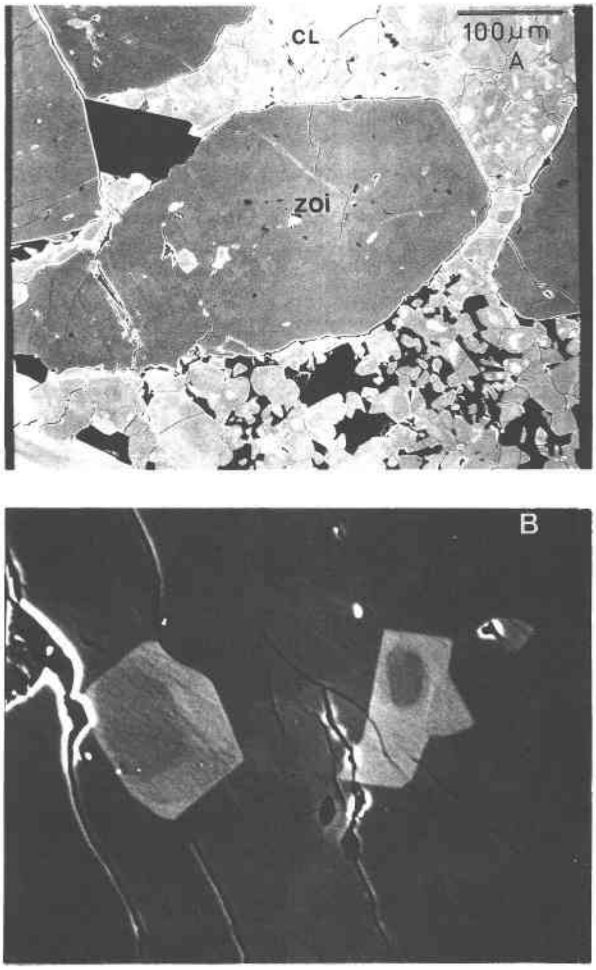

Fig. 10. (**A**) Backscattered electron image of zoisite and clinozoisite, together with albite (black, unlabeled), (**B**) 20-μm inclusions of clinozoisite in zoisite (close-up of the left central part of the zoisite crystal in **A**). Matrix and inclusion clinozoisite show the same type of zoning (sample RM71).

centimeter-sized zoisite crystals of the segregation are replaced along their rims by clinozoisite, paragonite, albite, and calcite, and adjacent to these newly formed minerals, zoisite changes its composition from 6–10 mol% Al_2Fe at the rim (cores are 11–15 mol%) to 16–21 mol%. The secondary clinozoisite ranges from 39 to 47 mol% Al_2Fe.

Samples FT-1 and DT-8 (Figs. 5, 9) are from the same area as sample St 1. They are both from banded eclogites (localities Frosnitztal, southern margin of the eclogite zone, and Dorfer Tal, western end of the Gastacher Wände). The eclogites experienced pressures near 2.0 GPa, at temperatures near 590 °C (Holland, 1979; Frank et al., 1987; Spear and Franz, 1986) with some subsequent reequilibration to lower greenschist facies conditions. The FT sample shows no signs of this reequilibration, whereas the DT sample is slightly retrograded (as indicated by the beginning of symplectite formation of some omphacite and the scattering of K_d values for garnet clinopyroxene). The mineral assemblage in both samples is epidote + garnet + omphacite + amphibole + phengite + dolomite + magnesite + rutile + quartz. Clinozoisite is in most cases strongly zoned with increasing Fe contents from core to rim; in coexisting zoisite the trend is similar but less pronounced. The zoisite composition ranges from 10 to 15 mol% Al_2Fe (one exception with 18 mol%), the clinozoisite from 34 to 52 mol%, with core compositions between 29 and 38 mol%. There are two average compositions of clinozoisite, one near 34, the other near 45 mol%. Figure 9 shows that omphacite inclusions are in textural equilibrium with both of these compositions. We use this observation to argue that the clinozoisite grains with the high Al_2Fe component are not late-stage overgrowths but rather formed during prograde metamorphism.

Sample RM 71 (Figs. 5, 10) is a garnet amphibolite with strong indications that it is a retrograded eclogite (symplectite of amphibole and plagioclase, corroded garnet; the main mineral assemblage is amphibole + plagioclase + chlorite + epidote + titanite). It comes from the basement complex of the Tauern Window, Maurer Tal. Eclogites within this basement record lower pressures (1.2

GPa) and temperatures (500 ± 50 °C; Zimmermann and Franz, 1989) than those within the eclogite zone. The coexisting zoisite-clinozoisite minerals occur in a small layer in the sample, coexisting with albite and garnet (± paragonite), with good indications for textural equilibrium. The zoisite crystals are embedded in clinozoisite and albite but also have inclusions of clinozoisite. These inclusions show the same type of zoning as the matrix clinozoisite, with very narrow rims of Fe-rich composition (42–54 mol% Al_2Fe), central parts with 31–34 mol% (Fig. 10b). This is again taken as an argument for prograde zoning of the minerals not modified by retrogression. The zoisite ranges from 8 to 16 mol% Al_2Fe, with core to rim zoning toward Fe-rich compositions.

Sample RW 103 (Fig. 5) is a calc-silicate nodule in an amphibolite. It comes from the Nubian Desert basement, approximately 30 km west of Delgo (20°N, Nile River) in the northern province of Sudan. This basement is characterized by a main stage of mineral formation in the upper amphibolite facies (*P* near 0.5 GPa, *T* near 650 °C), but contains relicts of granulite facies metamorphism (*P* = 0.8 GPa, temperatures near 800 °C; Bernau et al., 1987; Huth et al., 1984). The calc-silicate nodule consists of grossular + zoisite + diopside + anorthite + quartz, separated by a small reaction zone of clinozoisite + zoisite + diopside + anorthite from the amphibolite (mainly plagioclase + amphibole). Zoisite is strongly zoned from 2 to 12 mol% Al_2Fe, with Fe-rich rims, but zones of all compositions coexist with clinozoisite. The variations in clinozoisite composition (36–42 mol% Al_2Fe) occur in sharp zones parallel to the **b** axis. It is assumed that the zoisite formed during granulite facies conditions above the upper stability limit of clinozoisite, which is near 650 °C (Holdaway, 1972). During the amphibolite facies event, epidote component was formed, changing the zoisite composition and also forming separate clinozoisite crystals. Although both minerals are in grain contact and present in equal grain sizes, the large range in zoisite rim compositions coexisting with clinozoisite indicates disequilibrium.

DISCUSSION

A primary observation in nearly all of the samples that we have studied is that both zoisite and clinozoisite commonly show disequilibrium features, such as complex zoning patterns (especially in rocks of high-pressure origin), formation of texturally and chemically different types, and modifications of earlier minerals. Within a single grain the composition can vary widely and often irregularly, i.e., not parallel to the outer crystal faces. These variations in composition are controlled by mineral reactions producing epidote component in the rock and by crystal growth phenomena such as nucleation and growth rates. Intra- and intercrystalline exchange reactions seem to be of minor importance, and we conclude that volume diffusion in the epidote mineral group is slow. Another important factor influencing the compositional variations for coexisting minerals shown in Figure 5 may be the fact that minor elements can influence the width of the gap. This is evident for the REE (Fig. 5) and has also been shown for Sr by Maaskant (1985).

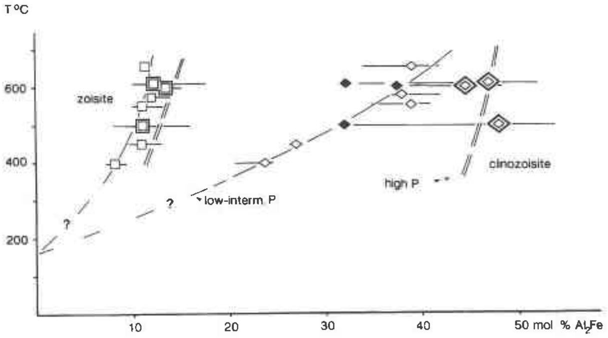

Fig. 11. *T-X* diagram based on analytical data in Figure 5 and text. The average values for several analyses are shown by the symbol; the horizontal line through the symbol gives the range of composition (compare with Fig. 5 for number of analysis pairs). Symbols with double lines refer to eclogites, and the double line labeled "high *P*" indicates the two-phase loop for high pressure. The solid symbols refer to the core compositions of the high pressure clinozoisite.

In Figure 11 we have arranged the data on coexisting clinozoisite-zoisite pairs (outer rim analyses) in a *T-X* diagram, using average values (mean of the analyses), but also showing the range of analyses, together with an estimate of the temperature of formation of the epidote minerals. The rocks were split into two groups, one with low to intermediate pressure of formation (<1 GPa), the other with high pressure (>1 GPa). These estimates are rather uncertain: even when rigorous thermobarometric calculations are made, the timing of equilibration of the epidote minerals is still unknown. Error boxes in the *T-X* diagram would be large, but several key features are evident despite these uncertainties: (1) The overall chemical variation in zoisite is much smaller than in clinozoisite, but both show an increasing Al_2Fe component with increasing temperature. This supports the previous findings of Enami and Banno (1980), Maaskant (1985), and Prunier and Hewitt (1985). (2) The largest compositional variations, in both zoisite and clinozoisite, were consistently observed in rocks of high-pressure origin. High-pressure rocks necessarily have a complex metamorphic history with more possible stages of mineral growth than, for example, during simple contact metamorphism. (3) Clinozoisite samples from the high-pressure terranes are significantly higher (by approximately 10 mol%) in Al_2Fe component than those from low-pressure terranes, although their estimated formation temperatures are similar. The same trend can be observed in Enami and Banno's (1980) data: Their FU and OM samples (their Fig. 4) come from low-pressure terranes, whereas their TO, NI, and IR samples are from eclogites; the compositional gap for the high-pressure rocks is significantly wider.

These observations provide evidence that pressure exerts an important influence on the position of the clino-

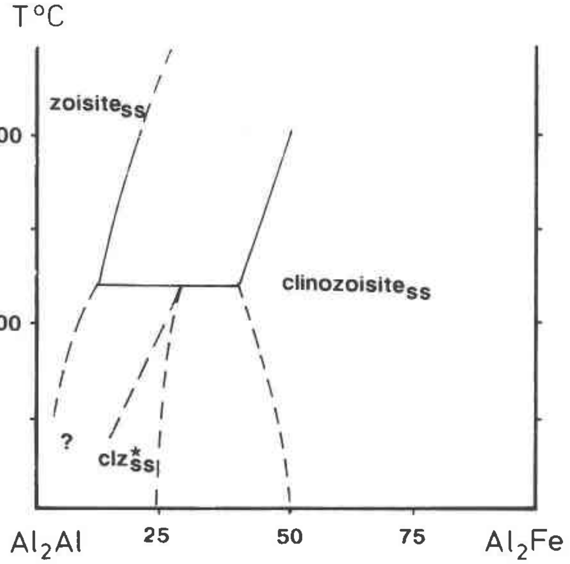

Fig. 12. Influence of a possible miscibility gap at low *T*, high *P*, as indicated by data of Selverstone and Spear (1985). A miscibility gap at low temperatures demands a second monoclinic variety labeled clz^*_{ss}.

zoisite limb. This is supported by observations of Spencer et al. (1988), who described pairs of zoisite and clinozoisite with 13–14 and 40–51 mol% Al_2Fe, respectively, from eclogites of the Western Gneiss Region (Norway), and Maaskant (1985), who reported a zoisite-clinozoisite pair (16.5 and 45 mol% Al_2Fe) from the high-pressure rocks of Galicia (northwestern Spain). We cannot distinguish unambiguously between the two possibilities discussed in Figure 2 because of the large variation in the compositions, but a configuration similar to Figure 2B seems quite likely.

At temperatures below approximately 400 °C the two-phase region is not well constrained. Our sample 1266 (see Fig. 5) shows that intermediate compositions for monoclinic crystals lying within the two-phase region at higher temperatures do exist. Therefore at low *P-T* conditions, the limb restricting the monoclinic phase area extends toward very Al-rich compositions, but its exact position is still uncertain. An equilibrium temperature for Reaction 1 near 200 °C at low pressures is likely, in agreement with calculations using the Berman (1988) data set and with the experimental determination of Jenkins et al. (1985).

The secondary epidote minerals formed in samples 85-1, 85-2, and St 1 show a large variation of compositions and textures within a single thin section, reflecting prolonged cooling of the rocks. The primary zoisite crystals with 10–12 mol% Al_2Fe were transformed during a hydrothermal event into grains with up to 26 mol%, typically without changing the morphology and the straight extinction of the crystal. The increasing Fe content is visible in narrow zones with increasing birefringence. Preliminary TEM data suggest that these zones consist of intergrowths of monoclinic and orthorhombic domains (Smelik and Franz, in preparation). Secondary clinozoisite crystals precipitated in cracks range from 30 to 54 mol%. This indicates that at low *P-T* conditions (approximately 0.3 GPa, 350 °C) no miscibility gap is apparent. The existence of almost Fe-free epidote minerals (symmetry not determined) in altered plagioclase, only a few micrometers away from the primary Fe-bearing zoisite and the secondary high-Fe clinozoisite, is typical of the disequilibrium preserved among neighboring grains of the epidote minerals. An orthorhombic symmetry of these Fe-free epidotes would be consistent with the transformation temperature for Reaction 1 near 200 °C, as mentioned above.

There is also evidence to suggest that miscibility gaps might occur in the monoclinic series at low temperatures or high pressures. Apparent miscibility gaps have been reported by several authors (Strens, 1965; Holdaway, 1972; Hietanen, 1974; Raith, 1976; Selverstone and Spear, 1985) on the basis of coexisting compositions of monoclinic epidotes in natural rocks. Our own analyses and backscattered electron images of epidotes show that disequilibrium textures are commonly preserved in single grains and even in coexisting monoclinic and orthorhombic forms; it is thus possible that published reports of miscibility gaps in the monoclinic series are merely an artifact of complex growth histories. On the other hand, such effects as ordering of Al and Fe^{3+} in M1 and M3 sites may create structural variations leading to miscibility gaps. We hope that detailed TEM studies will resolve this problem. Because most of the reported miscibility gaps are located at high Al_2Fe contents (between 35 and 75 mol%) and close at temperatures near 550 °C (Raith, 1976) or even lower (450 °C; Selverstone and Spear, 1985), they probably have no influence on the steep orthorhombic to monoclinic transformation loop reported here. However, if the clinozoisite limb is significantly shifted toward Fe-rich composition with increasing pressure, as indicated in Figure 11, the suggested monoclinic miscibility gaps might intersect the transformation loop. Such a configuration is shown in Figure 12 for the miscibility gap proposed by Selverstone and Spear (1985), with a critical temperature of 450 °C.

CONCLUSIONS

This study supports the previous findings of Enami and Banno (1980), Maaskant (1985), and Prunier and Hewitt (1985) that the transformation loop between clinozoisite and zoisite depends strongly on temperature and that Fe^{3+} (as well as the minor elements Ti, Mn, and Mg) is preferentially distributed into clinozoisite. In addition, we show that pressure may also be a significant variable and that in high-pressure rocks clinozoisite is enriched in Fe^{3+} compared to low-pressure rocks (at the same temperature, coexisting with zoisite) at intermediate temperatures between 400 and 600 °C; zoisite-clinozoisite relations remain uncertain at lower temperatures, although a narrowing of the compositional gap is likely, and at higher temperatures the upper stability limit of clinozoisite disturbs the simple binary phase relations.

The phase diagram that we present for the orthorhombic to monoclinic transformation can be used as an aid in the calculation of reactions involving epidote minerals. For example, if the pressure-sensitive reaction anorthite + H_2O = zoisite-clinozoisite + kyanite + quartz is considered, its position in a P-T diagram depends on the structural state, as well as on the composition of the epidotes. Calculations involving such a reaction at high P-T conditions (eclogite facies) should consider zoisite at bulk Al_2Fe compositions from 0 to 15 mol%, coexisting zoisite and clinozoisite in the range 15–45 mol% Al_2Fe, and clinozoisite only at Al_2Fe contents greater than 45 mol%. At low P-T conditions (greenschist to amphibolite facies) the compositional gap is small and of only minor effect. Hence, at these conditions clinozoisite should be used in the calculations for all bulk rock compositions that might yield more than 10–15 mol% Al_2Fe; zoisite would be the appropriate phase only for very Fe^{3+}-poor compositions.

For a more temperature-sensitive reaction such as lawsonite = zoisite + kyanite + quartz + H_2O, the pressure influence is more pronounced: at low P and T, 5–10 mol% Al_2Fe can be incorporated in zoisite, and the coexisting clinozoisite has around 20 mol%, whereas at low T and high P the clinozoisite has around 40 mol% Al_2Fe. The likelihood of forming zoisite in addition to clinozoisite increases with rising pressure because of the wider compositional gap. This provides an explanation for the relative abundance of zoisite in high-pressure rocks, although zoisite itself is also stable at low pressure.

Epidote minerals, owing to their stability over a wide range of P-T conditions, can be produced in many different stages during the metamorphism of a single rock; the apparently slow diffusion rates of Al $\rightleftharpoons$ Fe^{3+} exchange result in preservation of complex zoning patterns in individual grains. The epidote minerals thus have the potential to provide a wealth of petrologic information relevant, for example, to the reconstruction of P-T paths, provided that quantitative data on P-T-X relations in the epidote series are available. Though this is not yet the case, the empirical phase diagram presented in Figure 11 should serve as a starting point for future work. More analyses of coexisting mineral pairs from areas with well-known metamorphic histories are necessary to refine this diagram further. For fine-grained rocks, this will require simultaneous determination of crystal structure and chemical composition by transmission electron microscopy.

Ultimately, single epidote grains might be useful candidates for radiometric age determinations with a microbeam technique, both because they can contain high concentrations of trace elements such as REE, Sr, Pb, U, and Th and because they can record different stages of growth during complex metamorphic events; in this regard, they may eventually serve the same purpose in geochronologic studies of intermediate-temperature metamorphic rocks that zircon does in higher temperature (e.g., magmatic) rocks. Such studies have the possibility to yield timing information on the prograde paths of high-pressure rocks and thereby provide useful data for geodynamic studies of paleosubduction environments.

ACKNOWLEDGMENTS

The authors acknowledge a DFG grant Fr 557/3,4 (G.F.), a NATO travel grant (G.F. and J.S.), and an NSF grant EAR-8658145 (J.S.). Some of the sample material was collected on field trips supported by SFB 69. TEM work was carried out at Johns Hopkins University (Transmission Electron Microscopy Facility, supported by NSF grant EAR-8903630). G.F. gratefully acknowledges G. Smelik's help and introduction into TEM work, as well as the kind permission of D. Veblen to use his laboratory. We thank W. Heinrich, D. Hewitt, D. Jenkins, D. Lattard, G. Smelik and J.B. Thompson for discussions and critical reviews of the manuscript.

REFERENCES CITED

Abdel Rahman, E.M., Harms, U., Schandelmeier, H., Franz, G., Darbyshire, D.P.F., Horn, P., and Mueller-Sohnius, D. (1990) A new ophiolite occurrence in NW-Sudan—constraints on Late Proterozoic tectonism. Terra Nova, 2, 363–376.

Ackermand, D., and Raase, P. (1973) Coexisting zoisite and clinozoisite in biotite schists from the Hohe Tauern, Austria. Contributions to Mineralogy and Petrology, 42, 333–341.

Berman, R.G. (1988) Internally consistent thermodynamic data for minerals in the system Na_2O-K_2O-CaO-MgO-FeO-Fe_2O_3-Al_2O_3-SiO_2-TiO_2-H_2O-CO_2. Journal of Petrology, 29, 445–522.

Bernau, R., Darbyshire, D.P.F., Franz, G., Harms, U., Huth, A., Mansour, N., Pasteels, P., and Schandelmeier, H. (1987) Petrology, geochemistry and structural development of the Bir Safsaf-Aswan uplift, Southern Egypt. Journal of African Earth Sciences, 6, 79–90.

Bird, D.K., and Helgeson, H.C. (1980) Chemical interaction of aqueous solutions with epidote-feldspar mineral assemblage in geological systems. 1. Thermodynamic analysis of phase relations in the system CaO-FeO-Fe_2O_3-Al_2O_3-SiO_2-H_2O-CO_2. American Journal of Science, 280, 907–941.

Bird, D.K., Cho, M., Janik C.J., Liou, J.G., and Caruso, L.J. (1988) Compositional, order/disorder, and stable isotope characteristics of Al-Fe epidote, state 2-14 drill hole, Salton Sea geothermal system. Journal of Geophysical Research, 93, (B11), 13135–13144.

Deer, W.A., Howie, R.A., and Zussman, J. (1986) Rock-forming minerals, vol. 1B: Disilicates and ring silicates, p. 2–151. Longman, London.

Dollase, W.A. (1968) Refinement and comparison of the structures of zoisite and clinozoisite. American Mineralogist, 53, 1882–1898.

——— (1971) Refinement of the crystal structures of epidote, allanite and hancockite. American Mineralogist, 56, 447–464.

Enami, N., and Banno, S. (1980) Zoisite-clinozoisite relations in low- to medium-grade high-pressure rocks and their implications. Mineralogical Magazine, 43, 1005–1013.

Frank, W., Hoeck, V., and Miller, C. (1987) Metamorphic and tectonic history of the central Tauern Window. In H.W. Fluegel and P. Faupel, Eds., Geodynamics of the Eastern Alps, p. 1–418. Deuticke, Vienna.

Franz, G., Thomas, S., and Smith, D.C. (1986) High pressure phengite decomposition in the Weissenstein eclogite, Muenchberger Gneiss Massif, Germany. Contributions to Mineralogy and Petrology, 92, 71–85.

Ghose, S., and Tsang, T. (1971) Ordering of V^{2+}, Mn^{2+} and Fe^{3+} ions in zoisite $Ca_2Al_3Si_3O_{12}(OH)$. Science, 171, 374–376.

Gottschalk, M. (1990) Intern konsistente thermodynamische Daten im System SiO_2-Al_2O_3-CaO-MgO-K_2O-Na_2O-H_2O-CO_2, 272 p. Ph.D thesis, Universität Tübingen, Tübingen, Germany.

Hammerschmidt, K., and Franz, G. (1992) The influence of post-peak metamorphic alteration on 40 Ar/39 Ar white mica ages—a case study from the Münchberger Gneismasse, Germany. Contributions to Mineralogy and Petrology, in press.

Helgeson, H.C., Delany, J.M., Nesbitt, H.W., and Bird, D.K. (1978) Summary and critique of the thermodynamic properties of rock forming minerals. American Journal of Science, 278 A, 229.

Hietanen, A. (1974) Amphibole pairs, epidote minerals, chlorite, and plagioclase in metamorphic rocks, northern Sierra Nevada, California. American Mineralogist, 59, 22–40.

Holdaway, M.J. (1972) Thermal stability of Al-Fe epidote as a function of f_{O_2} and Fe content. Contributions to Mineralogy and Petrology, 37, 307–340.

Holland, T.J.B. (1979) High water activities in the generation of high pressure kyanite eclogites of the Tauern window, Austria. Journal of Geology, 87, 1–27.

Holland, T.J.B., and Powell, R. (1990) An enlarged and updated internally consistent thermodynamic dataset with uncertainties and correlations: The system K_2O-Na_2O-CaO-MgO-MnO-FeO-Fe_2O_3-Al_2O_3-TiO_2-SiO_2-C-H_2-O_2. Journal of Metamorphic Geology, 8, 89–124.

Hörmann, P.K., and Raith, M. (1971) Optische Daten, Gitterkonstanten, Dichte und magnetische Suszeptibilität von Al-Fe(III)-Epidoten. Neues Jahrbuch für Mineralogie Abhandlungen, 116, 41–60.

Huth, A., Franz, G., and Schandelmeier, H. (1984) Magmatic and metamorphic rocks of NW Sudan: A reconnaissance survey. Berliner geowissenschaftliche Abhandlungen (A), 50, 7–21.

Jenkins, D.M., Newton, R.C., and Goldsmith, J.R. (1985) Relative stability of Fe free zoisite and clinozoisite. Journal of Geology, 93, 663–672.

Johannes, W. (1985) The significance of experimental studies for the formation of migmatites. In J.R. Ashworth, Ed., Migmatites, 302 p. Blackie, Glasgow.

Klemd, R. (1989) P-T evolution and fluid inclusion characteristics of eclogites, Muenchberg Gneiss Complex, Germany. Contributions to Mineralogy and Petrology, 102, 221–229.

Langer, K., and Lattard, D. (1980) Identification of low-energy OH-valence vibration in zoisite. American Mineralogist, 65, 779–783.

Maaskant, P. (1985) The iron content and the optic axial angle in zoisite from Galicia, NW Spain. Mineralogical Magazine, 49, 97–100.

Myer, G.M. (1966) New data on zoisite and epidote. American Journal of Science, 264, 364–385.

Pistorius, C.W.F.T. (1961) Synthesis and lattice constants of pure zoisite and clinozoisite. Journal of Geology, 69, 604–609.

Prunier, A.R., and Hewitt, D.A. (1985) Experimental observations on coexisting zoisite and clinozoisite. American Mineralogist, 70, 375–378.

Raith, M. (1976) The Al-Fe(III) epidote miscibility gap in a metamorphic profile through the Penninic series of the Tauern Window, Austria. Contributions to Mineralogy and Petrology, 57, 99–117.

Ray, N.J., Putnis, A., and Gillet, P. (1986) Polytypic relationship between clinozoisite and zoisite. Bulletin de Minéralogie, 109, 667–685.

Seki, Y. (1959) Relation between chemical composition and lattice constants of epidote. American Mineralogist, 44, 720–730.

Selverstone, J., and Spear, F.S. (1985) Metamorphic P-T paths from pelitic schists and greenstones from the south-west Tauern Window, eastern Alps. Journal of Metamorphic Geology, 3, 439–465.

Spear, F.S., and Franz, G. (1986) P-T evolution of metasediments from the Eclogite Zone, south-central Tauern Window, Austria. Lithos, 19, 219–234.

Spencer, J.C., Valley, J.W., and Essene, E.J. (1988) Petrology of a margarite-bearing meta-anorthosite from Seljeneset, Nordfjord, western Norway: Implications for the P-T history of the Western Gneiss Region during Caledonian uplift. Lithos, 21, 117–128.

Strens, R.G.J. (1965) Stability relations of the Al-Fe epidotes. Mineralogical Magazine, 35, 464–475.

Thomas, S., and Franz, G. (1989) Kluftminerale und ihre Bildungsbeingungen in Gesteinen der Eklogitzone/Südvenedigergebiet (Hohe Tauern, Österreich). Mitteilungen der österreichischen geologischen Gesellschaft, 81, 189–218.

Tröger, W.E. (1982) Optische Bestimmung der gesteinsbildenden Minerale, Teil 1, p. 1–188. Schweizerbart'sche Verlagsbuchhandlung, Stuttgart.

Vogel, D.E., and Bahezre, C. (1965) The composition of partially zoned garnet and zoisite from Cabo Ortegal, NW Spain. Neues Jahrbuch für Mineralogie Monatshefte, 140–149.

Zimmermann, R., and Franz, G. (1989) Die Eklogite der unteren Schieferhülle; Frosnitztal/Südvenediger (Tauern, Österreich). Mitteilungen der österreichischen geologischen Gesellschaft, 81, 167–188.

MANUSCRIPT RECEIVED MAY 17, 1991
MANUSCRIPT ACCEPTED JANUARY 16, 1992